JOURNAL OF MATERIALS SCIENCE **36** (2001) 929–935

Hardness of titanium carbide films deposited on silicon by pulsed laser ablation

G. DE MARIA, D. FERRO
CNR Centro per la Termodinamica Chimica alle Alte Temperature, P.le A. Moro 5, 00185 Roma, Italy

L. D'ALESSIO, R. TEGHIL
Universitá della Basilicata, Via Nazario Sauro 85, 85100, Potenza, Italy

S. M. BARINOV
High Tech Ceramics Research Centre, Russian Academy of Sciences, Ozernaya 48, Moscow, 119361, Russia
E-mail: mnctk@cityline.ru

Hardness of titanium carbide films deposited on silicon (111) substrate by pulsed laser ablation is evaluated in dependence on laser beam fluence and the film thickness. Measurements were performed with the use of a common microhardness testing equipment, the indenter penetartion depth being more than thickness of the coating. Two methods based both on a law-of-mixtures approach were employed to calculate the film hardness from the measured hardness of the composite film-substrate system. One of them accounts for the indentation size effect. The hardness is revealed to reduce significantly with an increase of the film thickness and the laser beam fluence.

1. Introduction

Titanium carbide films have found wide application in various tribological engineering devices owing to its excellent hardness and, therefore, wear resistance. To apply titanium carbide coating on various substrates, physical vapour phase deposition (PVD) and chemical vapour phase deposition (CVD) methods are commonly employed [1]. An unique feature of non-equilibrium processing by pulse laser ablation deposition (PLAD) distinguishes it from other methods, because the energy of species ejected from the target is much larger than that in other evaporation methods [2, 3]. The structure of the as-deposited by PLAD method film is far from the thermodynamic equilibrium. This may principally result in some unusual effects in mechanical behaviour of the film.

One of the most important properties of the film that determines the service effectivity and reliability of the composite film-substrate system in tribilogical applications is the hardness. Hardness of bulk TiC is as high as 30 GPa [4]. Hardness of titanium carbide films deposited by PLAD has not been reported yet. One way to measure the hardness of thin films is an ultramicrohardness (nanoindentation) test [5, 6]. However, there is a problem related to the difficulty to obtain good reproducible experimental data because the contact scales are less than the film thickness, in our case the thickness being of some hundreds of nanometers. The applied load in such a test is usually less than 0.01N. The apparent hardness value varies with contact scale in this range, and the calculated hardness increases with a decrease in load. This effect is known as the indentation size effect (ISE) [7–10]. Therefore, if the hardness is used as a material selection criterion, it is clearly insufficient to quote a single hardness number obtained from the ultramicrohardness test. Besides, the precise measurements of the very small indenter prints is difficult to achieve in the ultramicrohardness tests range. So, there are problems to compare the ulramicrohardness data with those of microhardness test.

A different approach to measure the hardness of thin films is based on the microindentation of the film-substrate system at the indentation scale more to some extent than the film thickness, and on the calculation of the relative contributions of the substarte and the film to the hardness of the composite film-substrate system. This way allows probably to avoid the ISE, as has recently been demonstrated in [11]. The shortcomings of the models to calculate the film hardness from the film-substrate contact loading response were outlined in [12]. The present work is aimed at investigation of the hardness of thin TiC films deposited on silicon substrate by PLAD method in dependence on deposition conditions and film thickness from the results of a common microindentation test.

2. Experimental details

2.1. Deposition of films

The TiC films were deposited on polished silicon (111) substrate by the use of a PLAD apparatus that has been

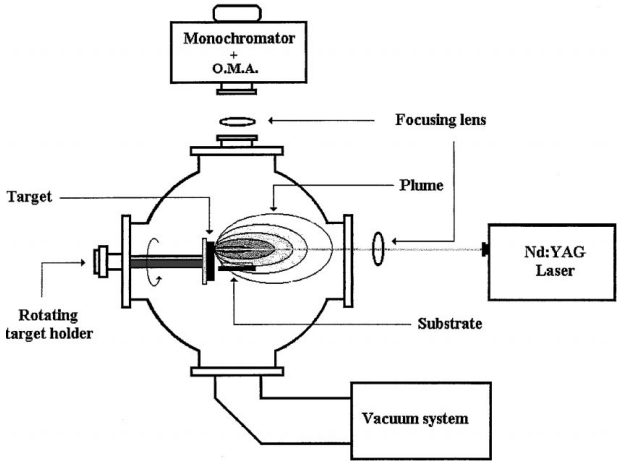

Figure 1 A scheme of the experimental assembly for PLAD.

described in details elsewhere [13], a scheme of the experimental assembly is given in Fig. 1. Hot pressed titanium carbide discs were used as targets. During the deposition, the silicon substrate was kept at room temperature. Deposition was carried out in a dynamic vacuum of 1.5×10^{-4} Pa. A frequency doubled Nd:YAG laser ($\lambda = 532$ nm, $\tau = 10$ ns, repetition rate 10 Hz) was utilized. The laser beam was oriented with an inclination angle of 45° with respect to the target, and the substrate was placed at distance of 25 mm from the target. The laser fluence was varied in the range from 5 to 15.7 J cm^{-2}. The deposition time was 1 h for all the specimens. The target was maintained in a rotation motion during the laser irradiation to minimize its craterisation.

The sampling is based on recent results obtained in an exhaustive study of the thermal behaviour of TiC in the laser ablation process [14]. It has been revealed that the ablation process and the film quality are strongly dependent on the beam fluence level. In particular, three fluence regions have been identified that originate films with distinct characteristics. The films obtained at fluences from 3.0 to about 8 J cm^{-2} are compact ones having a layered structure. The XPS surface analysis and X-ray diffraction patterns proved high composition stability with TiC stoichiometry equal to the target one (Ti/C = 1) [14]. Deposits prepared under higher fluence conditions have low quality owing to the numerous small fragments covering the surface. This is attributed to effect of target pieces expulsion, as clearly evidenced by SEM observations [14].

Microstructure and fractographic studies were performed using a scanning electron microscope Cambridge 100. Thickness of the deposited films was measured by SEM cross section observations. An absolute error of the thickness measurement was ±10 nm.

2.2. Hardness measurements

Hardness measurements were carried out using a Shimadzu HMV-2 Microhardness Tester (Shimadzu Corp., Japan) equipped with a standard Vickers pyramidal indenter (square-based diamond pyramide of face angle 136°). The hardness was calculated as the ratio of the applied load to the pyramidal contact area of the indentation:

$$H = \sin 68^\circ P/D^2 = 1.8544\, P/D^2 \qquad (1)$$

where P is the indentation load and D is the measured indentation diagonal. On each specimen indentations were made with 7 to 8 loads ranging from 0.245 to 19.614 N. Both diagonals were measured to diminish the effects of asimmetry on the imprint. Standard deviation of the diagonal measurements was about 5 to 9% of the diagonal length.

Because the thickness of the deposited films is very small ranging from 300 to 700 nm, the response of the film-substrate composite system to the indentation is supposed to be dependent strongly on the indentation severity. The depth of indenter penetration into the specimen is more than the film thickness, even at lowest load, so the "composite" hardness of the film-substrate system is obtained. Therefore, the relative contributions of the film and the substrate to the hardness have to be calculated. The models devised to separate the composite hardness on its constituents have been outlined in [12]. It was pointed out that it is difficult to construct a generalized model having soundly-based physical origin, which could allow to describe the contact response of the film-substrate system in an universal manner, taking into account various modes of deformation and fracture during the indentation process. A most common model is based on an area "law-of-mixtures" approach [15]. In the framework of this approach, the composite hardness H_c of the film-substrate system is expressed as

$$H_c = (A_f/A)H_f + (A_s/A)H_s \qquad (2)$$

where A is the contact area; H is hardness; subscripts f and s denote film and substrate, respectively; $A = A_f + A_s$ is the total contact area.

From the geometric considerations Equation 2 was specified as follows [9, 15, 16]

$$H_f = H_s + (H_c - H_s)\Big/\left[2c\left(\frac{t}{d}\right) - c^2\left(\frac{t}{d}\right)^2\right] \qquad (3)$$

where $c = 2\sin^2 11^\circ \approx 0.07$ for hard brittle film on softer substrate; d is the indentation depth (for the standard Vickers pyramide, the indentation depth is about one seventh of the diagonal length D [11]), and t is the film thickness. This equation has been derived under an assumption that $A_f/A = 2ct/d - c^2t^2/d^2$ and $A_s \approx A$. Therefore, the model is intended to be appleciable at large penetration depths where the surface displacement is more than thickness of the film. This corresponds generally to the experimental conditions in the present work.

The model does not consider the dependence of hardness on the load, known as an indentation size effect. The hardness variation with applied load can be introduced in Equation 3 through the relation between the

hardness and the reciprocal length of the indentation print as follows [7, 17]

$$H_f = H_{f0} + B_f/D \quad (4)$$

and

$$H_s = H_{s0} + B_s/D \quad (5)$$

where H_{f0} and H_{s0} are the intrinsic hardness of the film and substrate, respectively; B_f and B_s are constants, and D is the indentation diagonal length. Introducing relations 4a and 4b into Equation 3 and neglecting the second-order $1/D$ terms, the composite hardness becomes [16]:

$$H_c = H_{s0} + [B_s + 2c_1 t(H_{f0} - H_{s0})]/D \quad (6)$$

where $c_1 = c(D/d) \approx 0.5$ for the hard brittle film on a softer substrate system.

This equation is widely used to calculate the film hardness, and a reasonable fit of the results with the experimental data is generally achieved [16]. Particularly, the equation does hold well for indentation depths of more than the thickness of the film.

According to Equation 5, the experimental data on the hardness of the system film-substrate are plotted against $1/D$, and the intrinsic hardness of the film is calculated from the slope of the regression line taking into account the intrinsic hardness of the substrate which has to be evaluated from a separate test.

3. Results and discussion

The thickness of the films is dependent on the laser beam fluence during the PLAD process. The results of the thickness measurements are given in Table I.

Of course, some variations of the thickness occur across the film area owing to the leuticular shape of the coatings, and Table I gives the averaged value of thickness.

Scanning electron microscopy observations revealed that the films obtained with the fluence ranging from 5 up to 7.2 J cm^{-2} have a compact layered microstructure; X-ray photoelectron spectra indicated high compositional stability of the coating which being of Ti/C = 1 stoichiometry in this fluences range [14]. As the laser beam fluence increases, the quality of the film microstructure decreases owing to the numerous small fragments covering the surface [14]. These fragments are attributed to a mechanical effect of target pieces expulsion (spallation) by laser beam. These features can obviously influence the mechanical behaviour of the film.

TABLE I Thickness of films *versus* laser beam fluence

Specimen code	TiC5	TiC7	TiC8	TiC9	TiC16
Fluence, J cm^{-2}	5	6	6	7.2	15.7
Film thickness, nm	300	330	340	600	700

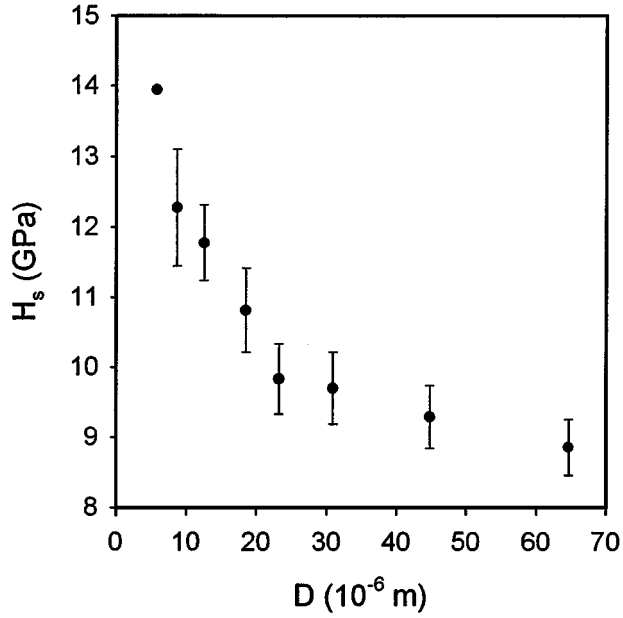

Figure 2 Hardness *versus* averaged imprint diagonal length for silicon (111) substrate.

Before to test the contact response of the film-substrate system, the indentation test on the uncoated silicon (111) substrate have been performed to evaluate the substrate intrinsic hardness. In Fig. 2 the hardness is plotted against the averaged diagonal length. It follows from these data that the calculated hardness diminishes with increasing imprint diagonal, this resulted from the indentation size effect (ISE). The reason for the ISE appears have been discussed in [10], particularly variation of the hardness with load is the result of the pill-up formation. We are really observed the pill-ups at the imprint on silicon (111).

Fig. 3 shows the dependence of the measured silicon hardness on the inverse of the imprint diagonal length. The plot is approximated well by a linear regression, according to Equation 4b. A least-squares fit of the plot to

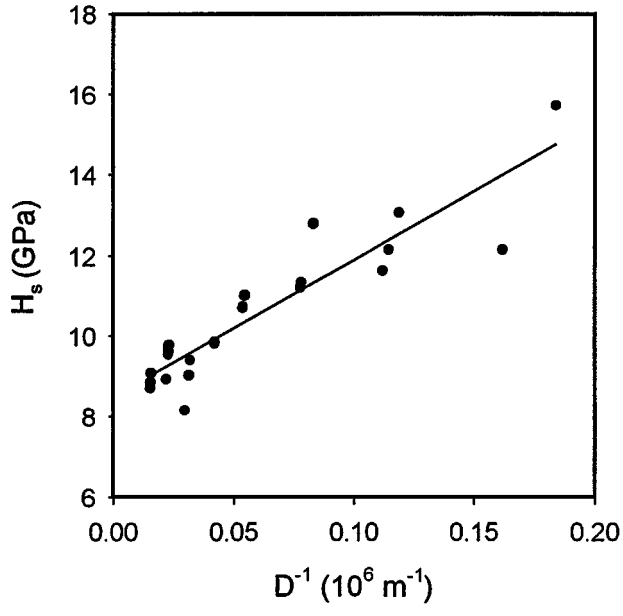

Figure 3 Hardness of silicon substrate *versus* inverse of imprint diagonal length.

Equation 4b gives H_{s0} and B_s be equal to about 8.5 GPa and 37.1×10^{-6} GPa/m, respectively. The value of the intrinsic hardness of silicon (111) of 8.5 GPa seems to be reasonable one.

During the microindentation tests of the composite film-substrate systems under investigation, the indenter penetration depth was always more than the thickness of the films, even at minimal indentation load of 0.245 N. Supposing the penetration depth equals to about 1/7 of the imprint diagonal length for a standard Vickers pyramidal indenter, the calculated values of the relative penetration depth, d/t, were varying from 2.3 at the load of 0.245 N to 25.0 at the load 19.614 N for the thinnest, of 300 nm film, and from 1.03 at the load of 0.245 N to 12.5 at the load of 19.614 N for the thickest, 700 nm thickness film. Therefore, the film contribution to the hardness of the composite system is expected to be small at high indentation loads, and consequently measured composite hardness will approach asymptotically the value of the intrinsic silicon substrate hardness.

Optical and scanning electron microscopy of imprints did not reveal the lateral cracks to be formed as well as the delamination of the film from the substrate when the indentation load was as small as of 0.245 N. An increase of the load to 2.942 N results in the delamination of the film that occurs at the side surfaces of the indenter, and in formation of large spalls. This kind of failure is shown in Fig. 4a. Further increase of the load to 19.614 N leads to the fracture of the substrate with the propagation of penny-shape cracks from the corners

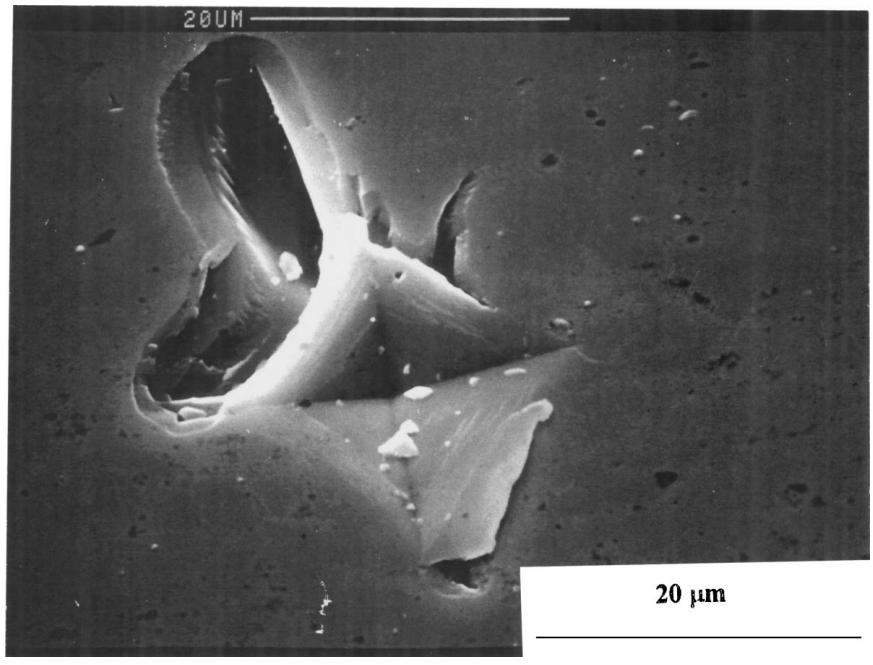

(a)

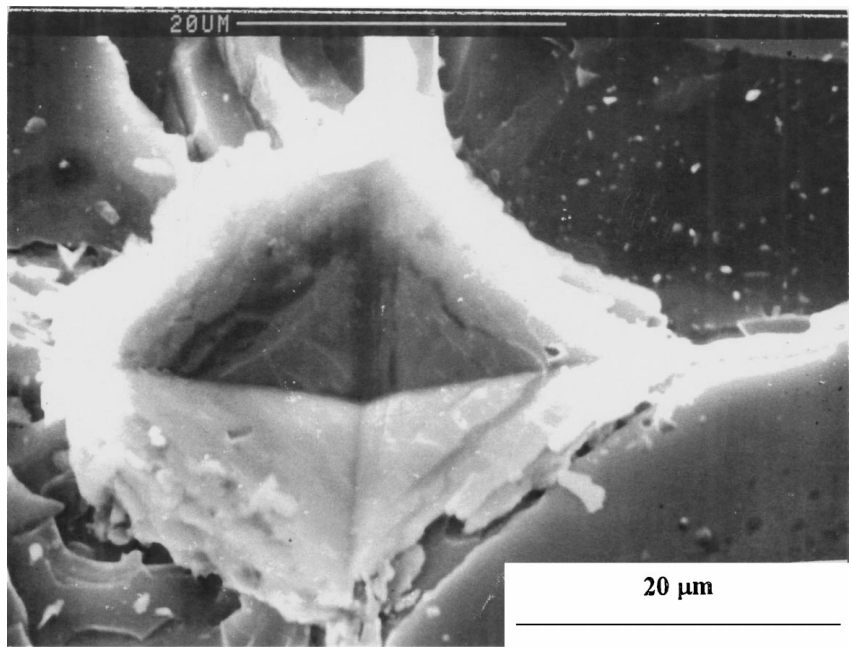

(b)

Figure 4 SEM micrographs of imprints onto TiC7 specimen.

of imprint (Fig. 4b). Generally, such behaviour of the film-substrate system under indentation corresponds to a model of the hard brittle film on a softer substrate where the film adjusts itself to the shape of the indentation by crack formation, as considered in [7, 11, 16]. Therefore, a constant c_1 in Equation 5 is reasonable accepted to be equal to about 0.5.

The hardness of the films has first of all been calculated from the experimental data using Equation 3 that does not hold for the ISE. The averaged results are shown in Fig. 5 where the calculated hardness is plotted against the imprint diagonal length. The indentation size effect is obvious. High scatter of the calculated values can be attributed to the effects of both the variation of the film thickness and the imprint diagonal measurement, on the second term of the Equation 3. It could be pointed out also that the second-order ct/d term of Equation 3 is small, especially at severe indentation loads, and can be neglected.

The following features of the plots in Fig. 5 can be pointed out. The calculated hardness values of the films are subjected to the ISE. This effect can be originated from the ISE for the substrate, as well as for the film. The second point is that the calculated data for the films TiC9 and TiC16 with highest thickness correspond to lower hardness values than these for thin films.

To evaluate the intrinsic hardness of the films, the composite hardness, H_c, of the film-substrate system are plotted against $1/D$, according to Equation 5 which allows to take into account the ISE. Examples of these plot are shown in Fig. 6 for the specimens of various film thickness. Experimental data are fitted well with a linear regression equation, the slope of the regression line being equal to $[B_s + 2c_1t(H_{f0} + H_{s0})] = B_c$, according to Equation 5. Estimated from these plots values of H_{s0} and B_c are given in Table II.

The value of H_{s0} calculated as an arithmetic mean from the above data is equal to 8.4 GPa that is in an excellent agreement with an independent evaluation of $H_{s0} = 8.5$ GPa obtained from the H_s *versus* $1/D$ plot for the uncoated silicon (111) substrate.

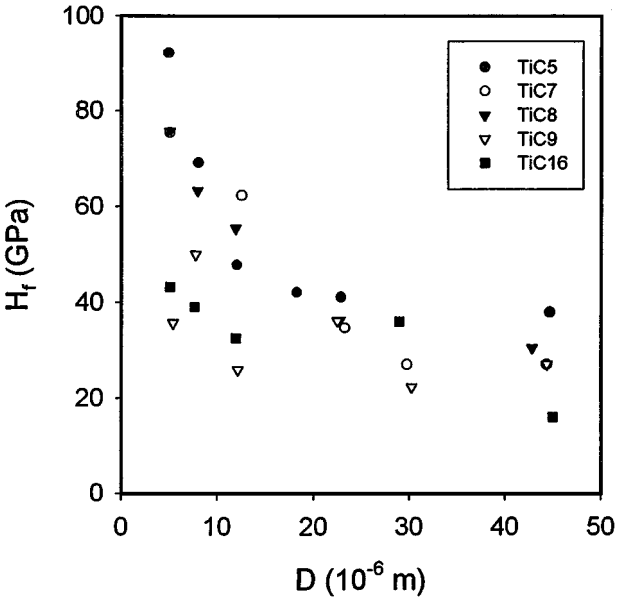

Figure 5 Hardness of films calculated by Equation 3 that does not hold for ISE.

TABLE II Estimated values of H_{c0} and B_c

Specimen code	TiC5	TiC7	TiC8	TiC9	TiC16
H_{c0}, GPa	8.8	8.3	8.9	7.9	8.0
B_c, 10^{-6} GPa/m	48.0	47.2	47.5	54.1	52.7

Fig. 7 shows the intrinsic hardness of TiC films which is estimated as $H_{f0} = H_{s0} + (B_c - B_s)/2c_1t$ in dependence on the film thickness. First of all, it could be noted that the hardness value for thickest film is in agreement with the data reported in a review paper [4] on hardness of bulk TiC, being equal to about 30 GPa. It can also be seen that the hardness depends on the film thickness. With an increase of the film thickness, the hardness decreases drastically. Such a trend can generally be explained by a non-uniformity of the films structure created at high laser beam fluence. It has particularly been shown that the TiC16 coating possesses non-uniform microstructure owing to the numerous of small fragments covering the surface [14].

The problem of size dependence of the mechanical properties of solids is generally in question. Very thin fibers and whiskers of various solids have, for example, strength which approaches the ideal strength [18]. The indentation process during hardness measurement is accompanied by the plastic deformation within a zone that is forming under indenter and, therefore, the hardness is supposed to be influenced by the yield stress behaviour. It is known well that the very thin crystals deform elastically until fracture begins, and the plastic deformation in these crystals is hampered [18]. This is due to the perfect structure of thin solids, e.g. lowered dislocations and planar defects density. Therefore, the film hardness is expected to be increased with a decrease of their thickness, like it does the yield stress for thin crystals. These general arguments are based on an analogy in the strength size effect for fibers, whiskers and films.

However, it should be noted that the authors of work [11] did not reveal the thickness dependence of the hardness of alumina films of 225, 325 and 360 nm thickness obtained on aluminium by anodic oxidation. Besides, the reported in [12] values of hardness for titanium nitride films deposited on steel by sputter ion plating (thickness range from 2 to 9.8 μm) and by plasma-assisted PVD method (0.48 to 23.9 μm) do not depend on the film thickness. Therefore, it can be supposed that the dependence of hardness of PLAD TiC film on their thickness is due to the microstructure formation features during the deposition process. These features have been reported in details in [14].

Shown in Fig. 8 is the dependence of the hardness on the laser beam fluence during the deposition. It should be noted that the hardness decreases significantly within the fluence range from 5 to 7.2 J cm^{-2} being lowered not so intensively as the fluence further increases. The fluence value of 7.2 J cm^{-2} is very close to the transition value from the real ablation mechanism to the target pieces propulsion, the boundary fluence between these mechanisms is reported to be equal to about 8 J cm^{-2} [14].

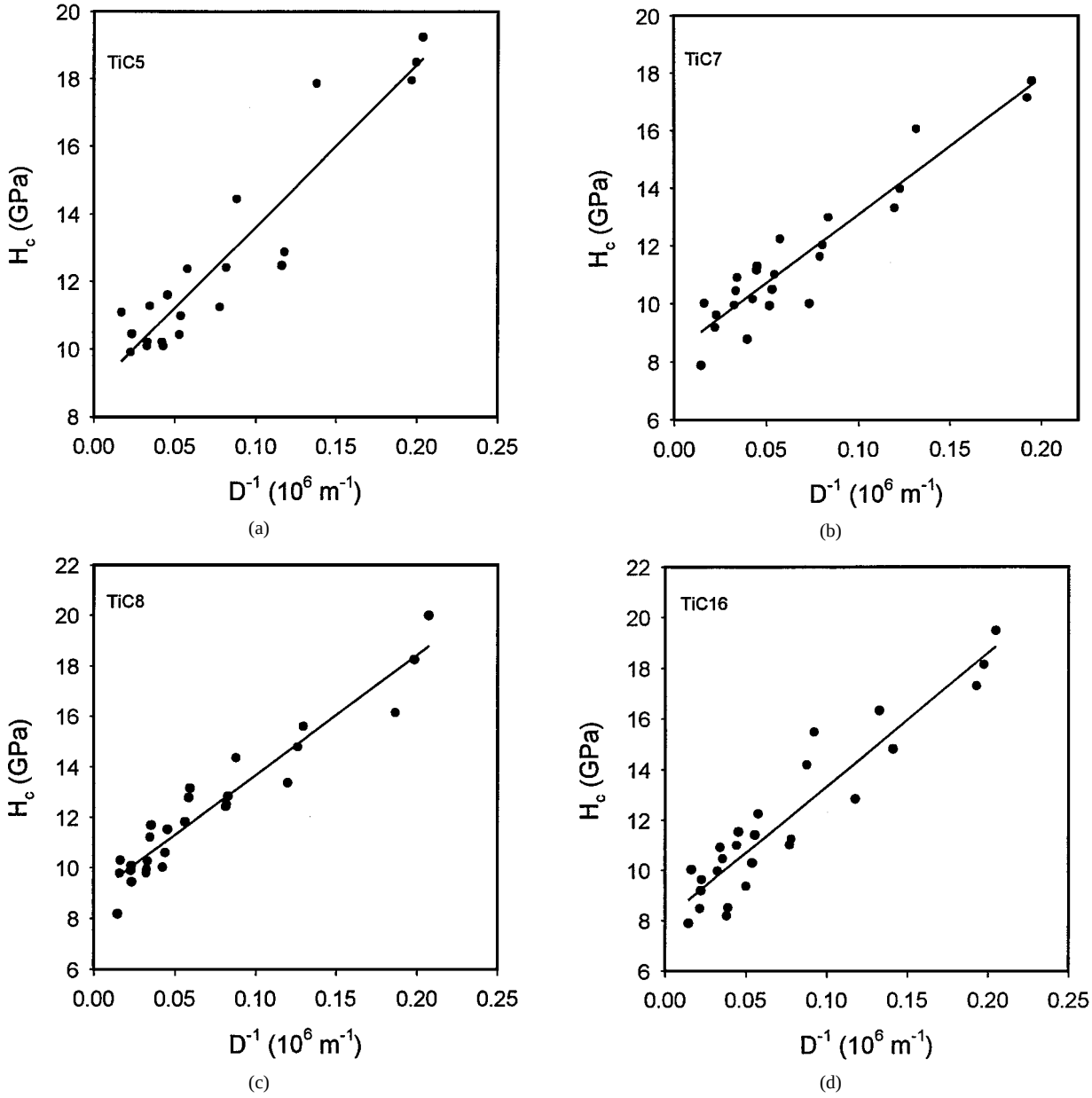

Figure 6 (a–d). Averaged composite hardness of film-substrate systems *versus* averaged inverse of imprint diagonal length.

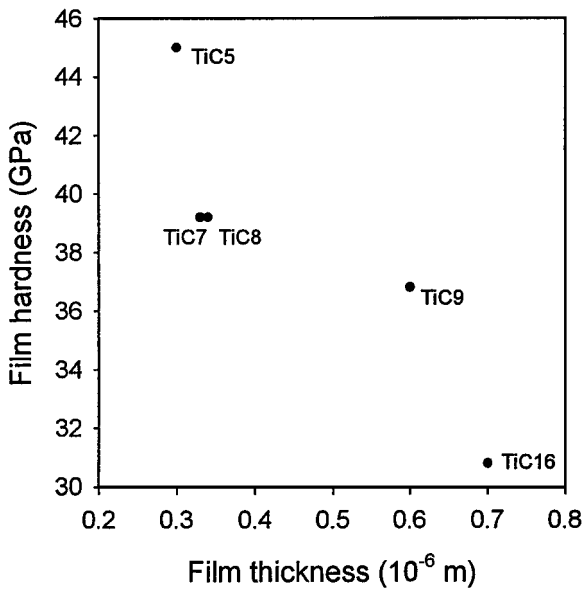

Figure 7 Dependence of hardness on film thickness.

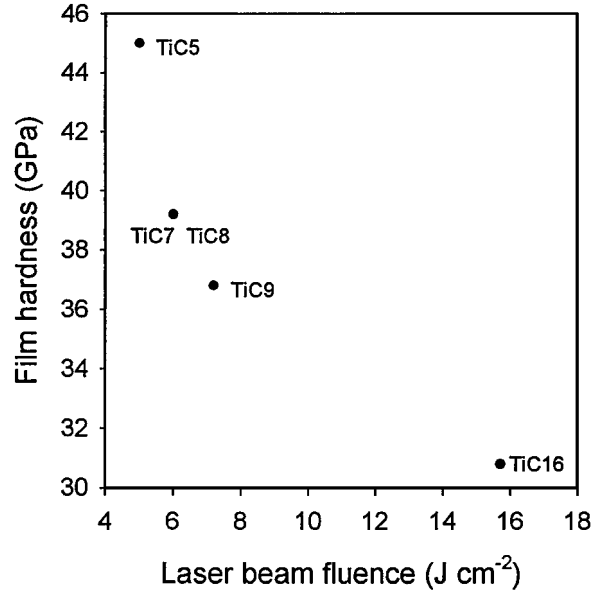

Figure 8 Dependence of hardness on laser beam fluence.

From the other hand, it could be keeping in mind that the structure of the films which is forming during the PLAD process is in a non-equilibrium state. Deposition of films by evaporation in vacuum results always in tensile stress imposed on the film due to the densification of the disordered to some extent structure that is "frozing" during the deposition [19]. If the ordering degree and, therefore, the tensile stress level are both dependent on the film thickness, so the hardness could be expected to be dependent on the film thickness too, just because tensile stress promotes cracking under the indentation. Obviously, a further study has to be performed to elucidate the microstructural features, disordering degree and stress state in the PLAD thin films in dependence of their thickness and the laser beam fluences to clarify the hardness size effect.

4. Conclusion

Experiments are performed with vacuum PLAD of titanium carbide films on silicon (111) substrate at the laser beam fluence of 5 to 15.7 J cm^{-2}, and the hardness of the films is measured in dependence on their thickness in the range from 300 to 700 nm. To measure the hardness, common microindentation tests were performed where the indenter penetration depth was always been more that the film thickness. The film hardness was separated from the composite hardness of the film-substrate system by the use of an approach based on an area law-of-mixtures model taking into account the indentation size effect. Reasonable values of the intrinsic film hardness are obtained. It is revealed that the film hardness is generally higher than that of bulk titanium carbide, and the hardness increases with a decrease of the film thickness. This is probably due to the conditions of the PLAD process resulting in variations of the structural features of the films.

Acknowledgement

The authors would like to thank Mr. G. Di Egidio for his contineous help in performing the experimental work. The microhardness tests were performed at ERNST S.p.r.l. (Varese, Italy), and the authors appreciate very much this opportunity. One of the authors, SMB, is grateful to the Landau Network - Centro Volta, The Italian Ministry of Foreign Affairs and Consiglio Nazionale delle Ricerche for supporting his participation in the work.

References

1. W. KERN and K. K. SCHUEGRAF, in "Handbook of Thin-film Deposition Processes and Techniques: Principles, Methods, Equipment and Applications," edited by Klaus K. Schuegraf (Noyes Publ., Park Ridge, 1988) p. 8.
2. O. RIST and P. T. MURRAY, *Mater. Lett.* **10** (1991) 323.
3. A. SANTAGATA, V. MAROTTA, L. D'ALESSIO, R. TEGHIL, D. FERRO and G. DE MARIA, *Appl. Surf. Sci.* **109/110** (1997) 376.
4. A. KRAJEWSKI, L. D'ALESSIO and G. DE MARIA, *Cryst. Res. Technol.* **33** (1998) 341.
5. Y. KINOSHITA and M. NISHIBORI, *Thin Solid Films* **148** (1987) 325.
6. P. J. BURNETT and D. S. RICKERBY, *ibid* **148** (1987) 41.
7. P. M. SARGENT, in "Microhardness Techniques in Materials Science and Engineering," ASTM STP 889, edited by P. J. Blau and B. R. Lawn (ASTM, Philadelphia, 1986) p. 160.
8. H. BUECKLE, in "Science of Hardness Testing and Its Research Applications," edited by J. H. Westbrook and H. Conrad (ASM, Metals Park, Ohio, 1971) ch. 33, p. 453.
9. O. VINGSBOO, S. HOGMARK, B. JÖNSSON and A. INGERMARSON, in "Microindentation Techniques in Materials Science and Engineering," edited by P. J. Blau and B. R. Lawn (ASTM, Philadelphia, 1986) p. 257.
10. A. IOST and R. BIGOT, *J. Mater. Sci.* **31** (1996) 3573.
11. V. NATRAVIL and V. STEJSKALOVA, *Phys. Status Solidi (a)* **157** (1996) 339.
12. A. M. KORSUNSKY, M. R. MCGURK, S. J. BULL and T. F. PAGE, *Surface and Coatings Technol.* **99** (1998) 171.
13. R. TEGHIL, A. GIARDINI GUIDONI, A. MELE, S. PICCIRILLO, M. CORENO, V. MAROTTA and T. M. DI PALMA, *Surf. Interf. Anal.* **22** (1994) 181.
14. L. D'ALESSIO, A. M. SALVI, R. TEGHIL, V. MAROTTA, A. SANTAGATA, B. BRUNETTI, D. FERRO and G. DE MARIA, *Appl. Surf. Science* **134** (1998) 53.
15. B. JÖNSSON and S. HOGMARK, *Thin Solid Films* **114** (1984) 257.
16. A. IOST and R. BIGOT, *Surface and Coatings Technol.* **80** (1996) 117.
17. F. FROELICH, P. GRAU and W. GRELLMANN, *Phys. Status Solidi (a)* **42** (1977) 79.
18. A. KELLY, "Strong Solids" (Clayderon Press, Oxford, 1973) p. 48.
19. J. A. THORNTON and D. W. HOFFMANN, *Thin Solid Films* **171** (1989) 5.

Received 29 November 1999
and accepted 12 April 2000